Letter

Origin of metal-insulator transitions in correlated perovskite metals

M. Chandler Bennett,[1,*] Guoxiang Hu,[2,3,†] Guangming Wang,[4] Olle Heinonen,[5] Paul R. C. Kent,[6] Jaron T. Krogel,[1,‡] and P. Ganesh[2,§]

[1]*Materials Science and Technology Division, Oak Ridge National Laboratory, Oak Ridge, Tennessee 37831, USA*
[2]*Center for Nanophase Materials Sciences, Oak Ridge National Laboratory, Oak Ridge, Tennessee 37831, USA*
[3]*Department of Chemistry and Biochemistry, Queens College, City University of New York, Flushing, New York 11367, USA*
[4]*Department of Physics, North Carolina State University, Raleigh, North Carolina 27695, USA*
[5]*Materials Science Division, Argonne National Laboratory, Chicago, Illinois 60439, USA*
[6]*Computational Sciences and Engineering Division, Oak Ridge National Laboratory, Oak Ridge, Tennessee 37831, USA*

(Received 16 July 2021; accepted 24 January 2022; published 5 April 2022)

The mechanisms that drive metal-to-insulator transitions (MIT) in correlated solids are not fully understood, though intricate couplings of charge, spin, orbital, and lattice degrees of freedom have been implicated. For example, the perovskite $SrCoO_3$ is a ferromagnetic metal, while the oxygen-deficient (*n*-doped) brownmillerite $SrCoO_{2.5}$ is an antiferromagnetic insulator. Given the magnetic and structural transitions that accompany the MIT, the driving force for such a MIT transition is unclear. We also observe that, interestingly, the perovskite metals $LaNiO_3$, $SrFeO_3$, and $SrCoO_3$ also undergo MIT when *n*-doped via high-to-low valence compositional changes, i.e., $Ni^{3+} \rightarrow Fe^{4+}$, $Sr^{2+} \rightarrow La^{3+}$, and $Sr^{2+} \rightarrow La^{3+}$, respectively. On the other hand, pressurizing the insulating brownmillerite $SrCoO_{2.5}$ phase drives a gap closing. Here we demonstrate that the ABO_3 perovskites most prone to MIT are self-hole-doped materials, reminiscent of a negative charge-transfer metal, using a combination of density functional and fixed-node diffusion quantum Monte Carlo calculations. Upon *n* doping the negative charge-transfer metallic phase, an underlying charge-lattice (or electron-phonon) coupling drives the metal to a charge and bond-disproportionated gapped insulating state, thereby achieving ligand-hole passivation at certain sites only. The size of the band gap is linearly correlated with the degree of hole passivation at these ligand sites. Further, metallization via pressure is also stabilized by a similar increase in the ligand hole, which in turn stabilizes the ferromagnetic coupling. These results suggest that the interaction that drives the band-gap opening to realize a MIT even in correlated metals is the charge-transfer energy, while it couples with the underlying phonons to enable the transition to the insulating phase. Other orderings (magnetic, charge, orbital etc.) driven by weaker interactions may assist gap openings at low doping levels, but it is the charge-transfer energy that predominantly determines the band gap, with a negative energy preferring the metallic phase. This *n* doping can be achieved by modulations in oxygen stoichiometry or metal composition or pressure. Hence, controlling the amount of the ligand hole, set by the charge-transfer energy, is the key factor in controlling MIT.

DOI: 10.1103/PhysRevResearch.4.L022005

I. INTRODUCTION

The metal-insulator transition (MIT) in various strongly correlated transition-metal oxides is essential for recently proposed device applications, for instance, memristors for next-generation neuromorphic computing [1–4]. However, understanding the underlying mechanism of the MIT in correlated solids has been a longstanding problem [5,6], making selection and optimization of appropriate materials difficult. The theoretical difficulty in analyzing these materials lies in the strong electron correlation, giving rise to complex many-body phenomena and a close coupling of charge, spin, orbital, and lattice degrees of freedom. Identification of the important variables and key interactions that influence the MIT in correlated metals has consequently remained elusive.

The ABO_x perovskite family has several candidate compounds that undergo a sharp and tunable MIT [7–11], which forms an excellent playground to look for the driving forces behind the transition. For example, consider the oxygen-rich perovskite $SrCoO_3$ (PV-SCO) which is a correlated ferromagnetic (FM) metal. The introduction of oxygen vacancies typically amounts to introducing negative charge carriers (i.e., *n* doping). In a conventional band-theory picture, such doping often increases electronic conductivity, but in PV-SCO it leads to an insulating ground state with a concomitant change in the magnetic ordering [12,13]. Indeed, the oxygen-deficient brownmillerite $SrCoO_{2.5}$ (BM-SCO) is an antiferromagnetic

*bennettcc@ornl.gov
†ghu@qc.cuny.edu
‡krogeljt@ornl.gov
§ganeshp@ornl.gov

insulator. However, under pressure (both uniform and uniaxial) this antiferromagnetic insulator shows a reduction in the electronic band gap by 40% [14]. Recent experiments [15] suggest that under pressure, the number of holes on oxygen ligands possibly increases, which in principle could stabilize a ferromagnetic coupling between the metal ions, in turn eventually closing the band gap in BM-SCO. Given the concomitance of the MIT to structural or magnetic transitions (or both), it is not immediately clear what would be the key change that triggers the MIT in PV-SCO and other similar correlated perovskite metals. Furthermore, it is not clear whether the gap opening is driven by Hubbard repulsive interactions from correlated electrons in the $3d$ orbitals, hybridization of orbitals between covalently bonded atoms, magnetic exchange interactions that favor Hund's rule, or charge-transfer energies that determine the transfer of electrons from the ligand (anion) to the metal (cation) sites.

The family of rare-earth nickelates is another example where the MIT occurs concomitantly with structural and magnetic transitions [16–18]. While the size of the rare earth tunes the transition temperature, the underlying mechanism appears to remain the same and is dependent on the metal-ligand bonding [19]. In all the nickelate compounds, the high-temperature phase is a correlated metal with fluctuating magnetic moments (i.e., the paramagnetic phase). Below a certain temperature, all compounds, except for $LaNiO_3$, transition into a bond-disproportionated phase, i.e., a phase with alternating long and short Ni-O bonds. Some compounds exhibit an additional transition to an antiferromagnetic (AFM) phase concomitant to this bond disproportionation. For example, recent experiments suggest even $LaNiO_3$ undergoes such an AFM transition below $\sim$157 K [20]. Similarly, n doping with hydrogen induces a metal-to-insulator transition in $SmNiO_3$, with the underlying mechanism still uncertain with the observation of local lattice distortions in the insulating phase [21,22]. Based on the Zaanen-Sawatzky-Allen (ZSA) classification scheme [23], the nickelates are self-hole-doped Mott insulators, where the self-hole doping is due to a negative charge-transfer energy.

Due to a forced high-valence cationic state (Ni^{3+}, d^7), the high-temperature metal is stabilized by self-hole doping (d^8L, where L indicates a ligand hole), and upon reducing the temperature, a *bond*-disproportionated insulating state emerges instead of a *charge*-ordered state, with short and long Ni-O bonds stabilizing alternating d^8L^2 and d^8L^0 Ni cations, that in some cases also stabilizes an antiferromagnetic ground state. As such, while a Hubbard repulsion is necessary, it is not sufficient to transition to an insulating phase. Indeed, even in conventionally well-regarded Mott insulators, such as VO_2 and NiO, and their superlattices, we recently demonstrated that the charge state of oxygen anions and its coupling to local structural distortions plays a significant role in driving the MIT [24–29]. But it is still not very clear why self-hole doping leads to a bond-disproportionated phase when temperature is reduced which opens a gap, and how the ZSA theory generalizes to MIT driven by changes in pressure, composition, and stoichiometry.

To address this question, we posit that the connection of the MIT and bond disproportionation extends beyond the nickelate family of perovskites and is not limited to MITs triggered by a change in temperature. Similar to the nickelates, the ferrates and the cobaltates have metal ions forced into high valency as well, e.g., Fe^{4+} in $SrFeO_3$ and Co^{4+} in $SrCoO_3$, and thereby possess large electron affinities, leading to a low, possibly negative charge-transfer [30,31] energy. Hence these systems should also exhibit self-hole doping to stabilize their metallic phase. We note that the MIT can also be triggered by compositional changes. Just as n doping PV-SCO by making it nonstoichiometric opens a band gap in the Brownmillerite phase, similarly n doping PV-SCO by substituting Sr^{2+} for La^{3+} also leads to a band-gap opening. Similarly, $LaFeO_3$ is an insulator and can be regarded as an n-doped PV-$SrFeO_3$ ($Sr^{2+} \rightarrow La^{3+}$). Given these observations, we hypothesize that metallic ABO_3 perovskites that demonstrate a MIT are self-hole-doped negative charge-transfer metals in the ZSA classification scheme. n doping such self-hole-doped metals fills these preexisting holes and gives rise to an insulating state, possibly via a charge-lattice (or equivalently, an electron-phonon) coupling, leading to a bond-disproportionated insulating structure that owing to a symmetry-lowering transition necessarily is also charge disproportionated (not necessarily charge-ordered). Magnetic ordering as well as other kinds of ordering, such as charge or orbital ordering, may further assist in the gap opening of this bond-disproportionated phase.

To prove the conjecture made above, in this work we use density functional theory–based methods together with the highly accurate, fixed-node diffusion Monte Carlo (FN-DMC) [32] flavor of quantum Monte Carlo (QMC) [33] to quantitatively compare the degree of self-hole doping in perovskite metals and how it correlates with changes in metal composition, oxygen stoichiometry, and pressure across a MIT. As a measure of the degree of self-hole doping, i.e., $d^{n+1}L$, we compare calculations of oxygen occupations via integrated densities around the oxygen sites. We additionally demonstrate that changes in the degree of self-hole doping triggers a charge-lattice instability. To benchmark our approach, we perform FN-DMC calculations of various ground-state properties and compare to experiments where possible, finding very good agreement. The ground-state properties used for comparison are the cohesive energies of the perovskite compounds—indicating the accuracy of describing atomic bonding—and the local magnetization around the metal site, which is important in determining the spin state of the metallic cation. A high-quality description of the ground state is foundational for our investigations of charge transfer in the perovskite family of materials considered here. The fundamental band gaps from FN-DMC–benchmarked DFT + U calculations are also in good agreement with available experimental gaps, with FN-DMC gaps showing similar trends across the different compounds. We find that holes are present in the oxygen site for correlated perovskite metals (as measured by the reduced oxygen occupations relative to the insulating compounds) and that transitioning to a gapped insulating phase via changes in metal composition or oxygen stoichiometry or pressure results in a reduction of the holes on oxygen sites (increased oxygen occupation). This is consistent with our density-of-states calculations, where the metals have an unoccupied p band, while insulators resulting from these metals undergoing an MIT have p-d–type band gaps. We find

strong evidence for the insulating phases to be bond disproportionated due to an underlying charge-lattice coupling. We therefore prove our conjecture that self-hole-doped correlated metals can trigger a metal-to-insulator transition by n doping into their unsaturated holes (increased oxygen occupation) due to a strong charge-lattice (or electron-phonon) coupling in perovskites, and that this n doping can be achieved by changes in oxygen stoichiometry, metal composition, or pressure. Hence, controlling the ligand-hole population, set by the charge-transfer energy, is the key factor in controlling MIT, even in correlated perovskite metals with strong on-site Hubbard interactions.

II. RESULTS & DISCUSSION

We perform a combined study using density functional theory (DFT) with a linear-response determined Hubbard U (i.e., U_{LR}) [34] as well as fixed-node diffusion Monte Carlo calculations to obtain ground-state properties. Computations were performed for metallic $SrCoO_3$ and $LaNiO_3$ compounds as well as the insulating $LaFeO_3$ and $LaCrO_3$ compounds in the perovskite phase and $SrCoO_{2.5}$ in the brownmillerite phase, at pressures ranging from 0 to 8 GPa. Further details are provided in the Supplemental Material [35].

A. Implications of ground-state energies and magnetic structure

Tables VIII and IX in the Supplemental Material [35] compare the cohesive energies and the local moments computed from FN-DMC to available experiments, respectively. Cohesive energy has contributions from all necessary interactions and is often incorrect in standard DFT calculations [36]. Here we find that the cohesive energies for $LaNiO_3$, $LaFeO_3$, and $LaCrO_3$ are in good agreement with estimates from the literature (derivations of experimental cohesive energies are provided in the Supplemental Material, SM). Particularly, we find that the inclusion of spin polarization is necessary to bring the cohesion of $LaNiO_3$ in closer agreement with experimental estimates, suggesting that the physics that stabilizes the local moment is essential in describing its electronically metallic state. The accuracy in cohesive energies for both metals and insulators indicates that FN-DMC is appropriate for looking at the driving force behind the MIT. In addition to cohesive energies, the methodology also captures the magnitude of the local moments and its change with coordination and structure type for the cobaltates, with absolute values very close to the values obtained from spin-polarized neutron-scattering experiments in the literature [20,37,38]. This affirms our methodology to predict the underlying electronic structure, allowing us to meaningfully conclude from systematic changes observed in charge or spin densities and derived quantities computed from the FN-DMC–estimated many-body ground-state wave function.

Rhombohedral $LaNiO_3$ was thought to be a paramagnet, until very recent experiments on single crystals of $LaNiO_3$ demonstrated that it undergoes a transition to an antiferromagnetic phase below $\sim$157 K while still remaining metallic [20]. Nevertheless, the measured local moment was $\sim 0.3\mu_B$, much smaller than the moments on other perovskite systems, in good qualitative agreement with trends observed from our FN-DMC calculations, which even in the ferromagnetic phase of rhombohedral $LaNiO_3$ finds a lower moment of $\sim 1.02\mu_B$ (SM Table IX) compared to other perovskite magnets. Note that our FN-DMC moment for the G-type AFM ordering of $LaNiO_3$ was also small ($\sim 0.52\mu_B$); however, this ordering was not energetically favored in FN-DMC over FM ordering. In all cases we have used spin-symmetry-broken trial wave functions in FN-DMC, which may partially explain the larger fluctuations observed when the predicted moments are small in magnitude. The local moments of all other compounds from our fully *ab initio* DMC calculations, including those on the different Wyckoff positions for the Brownmillerite phase, show excellent agreement with experiments.

The on-site moments may be understood qualitatively in the atomic limit as $\sim 2\sqrt{s(s+1)}$, where s is the spin multiplicity, so we find that the metal sites under an octahedral crystal-field splitting are close to a high-spin configuration for $LaCrO_3$ ($t_{2g}^3 e_g^0$) and $LaFeO_3$ ($t_{2g}^3 e_g^2$), an intermediate spin state for $SrCoO_3$ ($t_{2g}^4 e_g^1$), and a low-spin state for $LaNiO_3$ ($t_{2g}^6 e_g^1$). Interestingly, both linear-response theory as well as FN-DMC orbital optimization predict an increasing trend in the strength of the on-site Hubbard repulsion for $3d$ electrons as we increase the d-orbital filling from $LaCrO_3$ to $LaFeO_3$, but it is reduced slightly as we move to SCO and LNO (details in SM [35]). But the variation overall is not large, and both the U_{LR} and the U_{DMC} remain between 4 and 5.5 eV. Further, the band gaps do not follow the trend of the Hubbard interaction, with $LaCrO_3$ having a larger gap than LFO, and the SCO with a similar value for the Hubbard interaction as $LaCrO_3$, showing a metallic phase. This suggests that while the Hubbard interaction parameter (including the magnetic exchange, which dictates the Hund's rule) is necessary to stabilize the spin state and determine the local moment, the opening of the band gap is determined in large measure by other interactions, such as charge transfer. Further, the responsible interaction necessarily also destabilizes the high-spin state favored by Hund's rule in both SCO and LNO. Because all compounds have the same oxygen ligand, one way to assess the degree and nature of charge transfer across these compounds is to compare the charge associated with it.

B. Understanding key ligand charge behavior

To understand what type of charge transfer could be present in our systems, we next compare the charges on the oxygen ligand sites. The charges were computed by integrating the radial charge density around oxygen atoms within a fixed radius for all compounds, from both the linear-response LDA + U_{LR} as well as the FN-DMC following a nodal optimization using LDA + U orbitals. The computed charges are in good agreement between the different methods (see SM Tables III–V [35]), suggesting that the linear response captures the bonding characters in the solid appreciably well. As also seen in Fig. 1, the LDA + U_{LR} band gaps are in decent agreement with the experimental gaps. A high degree of charge transfer from oxygen ligands to the metal site is indicative of a negative charge-transfer energy. This is what we observe from Figs. 1(a) and 1(b), where the metallic SCO and LNO are seen to have the lowest relative charges on the oxygen atoms compared to the mean or majority charges carried by the

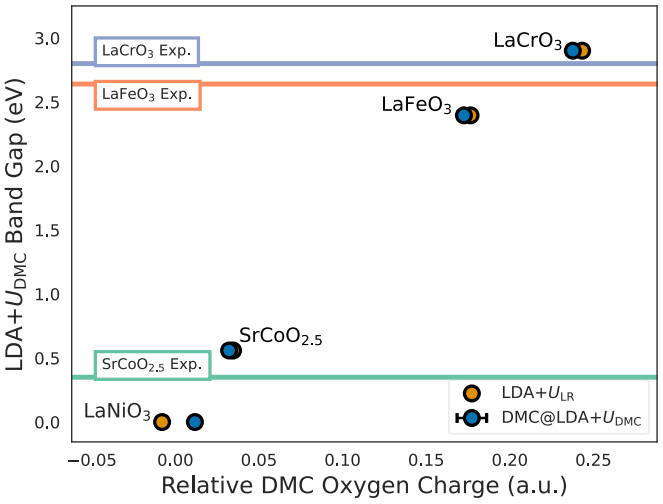

(a)

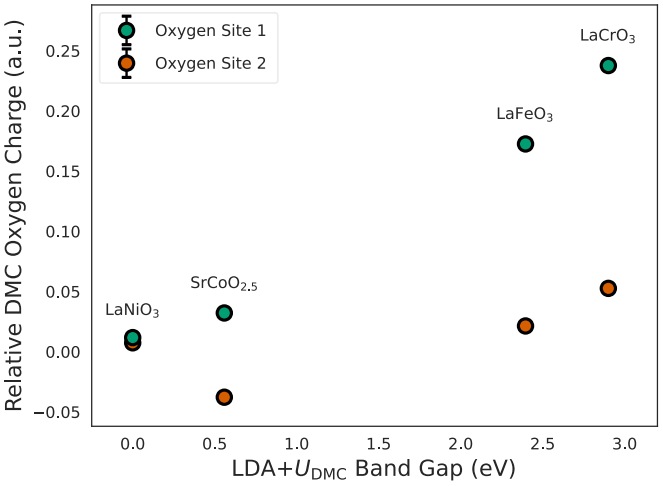

(b)

FIG. 1. (a) For $LaNiO_3$, $SrCoO_{2.5}$, $LaFeO_3$, and $LaCrO_3$, optical band gaps calculated within LDA + U vs the DMC cumulative radially averaged charge around the oxygen site relative to $SrCoO_3$ (with O charge 6.4120 a.u.). The oxygen site with majority charge was used for each system, and the value of U that minimizes the FN-DMC energy is chosen for each system. Cumulative charges are also shown from LDA + U, with U values consistent with DMC. For comparison, we indicate experimentally measured band gaps for the insulating systems ($SrCoO_{2.5}$ [13], $LaFeO_3$ [39], and $LaCrO_3$ [40]) with horizontal solid lines. (b) LDA + U_{DMC} band gap vs site-specific cumulative radially averaged charge around the oxygen site relative to $SrCoO_3$.

oxygen ligand among all the compounds. Interestingly, the change in the majority charge on the oxygen ligand correlates linearly with the band gap, irrespective of whether we consider the observed experimental gap or the band gaps calculated via LDA + U_{LR} or LDA + U_{DMC}, and in spite of the change in the structure from perovskite to a brownmillerite phase. This clearly suggests that the quantity determining the size of the band gap across MIT in correlated perovskites is the charge-transfer energy, and that the metals are self-hole-doped because it is negative.

A negative charge-transfer energy will also lead to a change in the formal oxidation state of the metal site and thereby the magnetic moment. For example, in PV-SCO, the nominal Co^{4+} ($3d^5$) valency will get lowered due to a transfer of electron from the ligand to the metal-site, destabilizing the nominally high-spin $t_{2g}^3 e_g^2$ state and giving rise to an intermediate spin state $t_{2g}^4 e_g^1$ with a net moment less than $\sim 3\mu_B$, which would be in good agreement with both experiments and our calculations (SM Table IX). Our integrated charges around the Co site also support this conclusion, with the nominal valency of ~2.65 a.u., closer to a Co^{3+} as shown in Table SM-I. Similarly, hole doping is seen to lower the nominal Ni^{3+} to be ~1.73 a.u., closer to Ni^{2+}. With a reduced valency, it would be possible to stabilize a low-spin state, such as $t_{2g}^6 e_g^2$, explaining the low moments in both the measured and our computed values. Note that this would also require the holes to have an e_g symmetry so as to quench the high-spin moments in the e_g subbands of the Co and Ni atoms. As we will see below, this is just what we observe.

While the nominal charges are much reduced for the metallic PV-SCO and PV-LNO, consistent with a negative charge-transfer picture, the insulating perovskites have a charge state closer to the nominal valency, e.g., a valency of 3+ in $LaFeO_3$ (2.50 a.u.) and $LaCrO_3$ (2.78 a.u.) (Table SM-I). Nominally, an isolated oxygen atom possesses 6 a.u. of charge. We note that our pseudopotentials use a two-electron core for oxygen and a ten-electron core for the 3d metals. Due to formation of metal-ligand bonding and owing to its high electronegativity, oxygen atoms are seen to possess more than 6 a.u. of charge for the compounds. Remarkably, the amount of oxygen-ligand charge appears to be the same (6.41 a.u.) for the two metallic systems–PV-SCO and PV-LNO, even though the total charges on the metal sites (Co and Ni) are very different (14.35 and 16.27 a.u.) (see Table SM-II). This again underscores the importance of the anion O-p states in determining the overall electronic structure. Magnetic transitions could in certain cases result from a MIT, such as in PV-SCO, but do not primarily drive it. Indeed, even $LaNiO_3$ was found to be a metal, a rarity for a material with an AFM ground state, consistent with experiments. This difference relative to broadly observed FM correlated metals suggests that modified magnetic interactions that could result in a particular type of AFM ordering for $LaNiO_3$ and FM for other materials may not be the primary determinant for gap openings in self-hole-doped perovskite metals. Given that the gap varies monotonically with the formal electronegativity of the metal atom (see Fig. SM-1), it is clear that the opening of the gap in these self-hole-doped metals would require changing the nature of this charge-transfer energy, i.e., making it more positive as the gap increases.

To investigate how the nature of the gap changes, we look at the orbitals participating in the gap opening. If there is an energy cost to transfer charges from the O-p orbitals to the metal-d orbitals, then the system would be gapped. Such a gap is naturally realized when the Fermi level moves from the middle of the O-p band, such as the case in the self-hole-doped metals, to the top of the O-p-band, giving rise

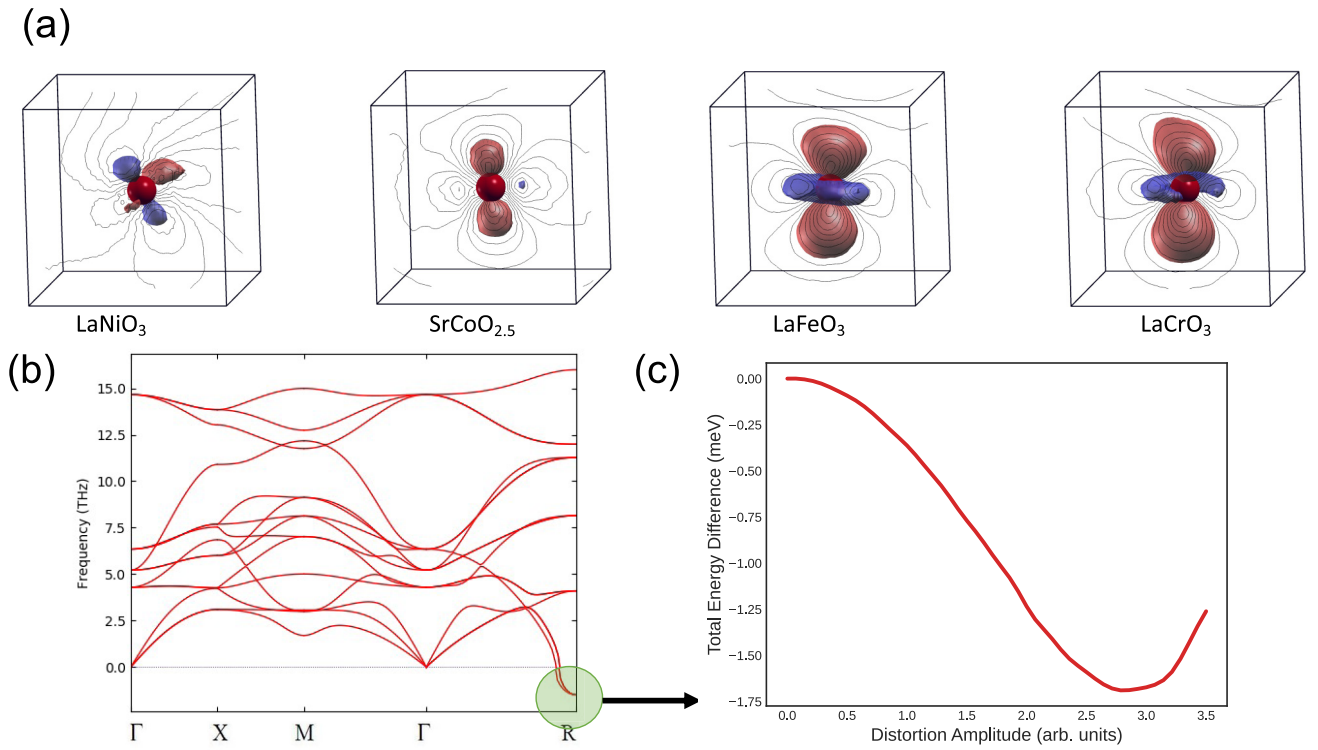

FIG. 2. (a) DMC charge-density isosurface differences for the indicated compounds with respect to PV-SCO plotted around an apical O atom. An increase in charge is shown in red while a decrease in blue. For each of the isosurfaces, the oxygen atom is centered in a cube of length 1.4 Å, and we take an isovalue of 0.022 a.u. so that each graphic can be soundly compared. (b) Phonon bands for e^--doped PV-SCO showing dynamic instability at the R point corresponding to an octahedral rotation. (c) Energy surface along the distortion corresponding to the instability at the R point suggesting a tendency for bond disproportionation due to charge disproportionation.

to a p-d type gap. A larger Hubbard interaction would naturally yield a larger p-d gap. Indeed, as shown in the calculated projected density of states, Fig. SM-2 in the Supplemental Material [35], both metallic SCO and LNO show a relatively large number of states with an O-p character at the Fermi level. As we move out of this metallic phase by reducing the amount of charge transfer from O-p to the metallic d state, by stoichiometrically or compositionally n doping it, a gap is opened in the insulators BM-SCO (Fig. 3) and $LaFeO_3$ (Fig. SM-2). These compounds show a p-d type band gap, reminiscent of a more positive charge-transfer system. As we further move to $LaCrO_3$, the amount of charge on the ligand site further increases, with the Cr metal showing a more formal oxidation state of $+3$, as noted above. At this point the band gap is equally determined by the Hubbard interaction and the charge-transfer energy, as also evidenced in the increased d contribution to the valence state in the projected density of states (Fig. SM-2).

The charge difference with respect to a self-hole-doped metal indicates how the density would respond to electron doping such a metal and represents the nature of the lowest excitation. This is clearly seen when we plot the DMC charge-density isosurfaces, localized around the oxygen sites as shown in Fig. 2(a) for the different compounds, in reference to the metallic PV-SCO. While the difference between metallic LNO and SCO shows the hole to have more of a t_{2g} symmetry, the gapped insulators show the hole state to have more of an e_g symmetry. This is exactly what we expect, because for the self-hole doping to destabilize the high-spin states in the metallic SCO and LNO, as discussed above, the states involved in the electron transfer need to have an e_g symmetry. Further, with increasing n doping the magnitude of this charge transfer increases, suggesting that the charge-transfer energy is becoming more positive. Thinking of this charge-density difference as the lowest type of excitation from the sea of electrons in the self-hole-doped metal to form an n-doped insulator, we see that the nature of this excitation is p-d-like, in agreement with the predominantly p-d-like gaps we observe for all systems in their density of states (Fig. SM-2). These observations suggest that n doping a negative charge-transfer metal can result in making the charge-transfer energy more positive. However, it is not clear if n doping simply shifts the Fermi level to open a band gap when the Fermi level reaches the top of the p band or if there is some kind of instability that opens a gap when the system is perturbed away from its self-doped metallic state.

Notice that while the majority charge on the oxygen ligand showed a monotonic increase with n doping the self-hole-doped metal, the compounds show a symmetry-lowering transition, which we can also associate with *charge* disproportionation. Indeed, while one of the oxygen-ligand site shows an increase in charge [Fig. 1(b)], the others have the same electron count as in the metallic phase. Also, a *shorter* metal-ligand bond length is associated with an oxygen site with *less* charge in all the compounds we have investigated, as shown in Table SM-IV. This suggests a clear connection between

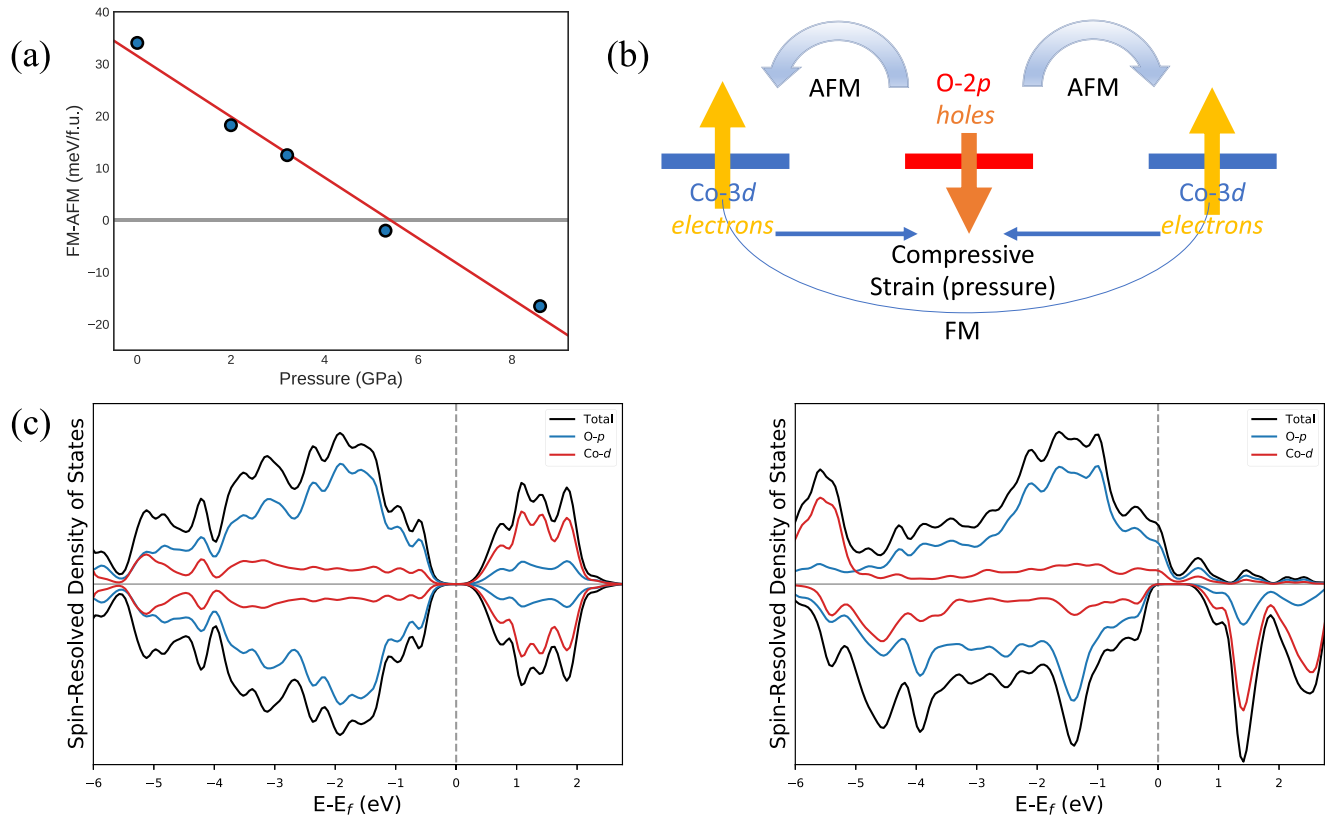

FIG. 3. (a) LDA + U enthalpy difference in BM-SCO as a function of strain. (b) Scheme of how holes mediate the magnetic transition. (c) LDA + U DOS plots of AFM insulator and FM metal phases of BM-SCO.

charge and bond disproportionation. Interestingly enough, as the band gap increases, the amplitude of the charge disproportionation also increases. Without further information, it is not immediately clear if the charge disproportion is caused by the bond disproportionation or vice versa, and what if any is its role in opening the band gap. But it is clear that under n doping when a self-hole-doped metal undergoes an insulating transition, symmetry is always lowered.

C. Charge-lattice coupling in $SrCoO_3$

To further understand this connection between charge and bond disproportionation and explain the symmetry lowering, we subjected cubic $SrCoO_3$ to the same level of electron doping (0.25 e^-/Co) as the largest radial charge transfer we observed in our study. Interestingly, as shown in Fig. 2(b), n-doped PV-SCO shows a phonon instability. The instability is at an R point of the Brillouin zone, corresponding to an octahedral rotation. Indeed, a similar R-type octahedral rotation underlies the ground-state structure of $LaFeO_3$, leading to its rhombohedral symmetry. Freezing the octahedral rotation lowers the energy, as seen in Fig. 2(c), suggesting a weak but persistent charge-lattice (i.e., electron-phonon) coupling. Similarly, hole-doping $LaFeO_3$ also gives rise to a phonon instability (Fig. SM-3). This suggests that as the correlated metal becomes n-doped, either via removing oxygen atoms or chemical substitution (or by applying strain as discussed below), the system undergoes bond disproportionation due to the underlying charge-lattice coupling, which in turn can lead to a charge-disproportionated state as the symmetry gets lowered. Indeed, even in hole-doped correlated metals that show a charge-ordered ground state, phonon damping and changes in heat conduction have been experimentally observed, supporting this thesis [41]. Such bond and charge disproportionation can remove electronic degeneracies and stabilize other symmetry-breaking transitions such as magnetic, charge-ordering or orbital-ordering, eventually opening a band gap. While we demonstrated how a self-hole-doped metal can become an insulator due to change in metal composition and oxygen stoichiometry, pressure can achieve the same result. Indeed, a recent experiment suggests that pressurizing the antiferromagnetic BM-SCO phase leads to a reduction in the band gap [14]. While beyond 8.5 GPa the system appeared to transform into a different structure, up to 8.5 GPa a monotonic reduction in the optical gap was seen with pressure without any structural change. Indeed, BM-SCO is an insulator in the antiferromagnetic phase but a metal in the ferromagnetic phase, as seen in our density-of-states plot in Fig. 3(c). By plotting the enthalpy difference between the two magnetic orderings as a function of strain induced by pressure [Fig. 3(a)], we find that the FM ordering becomes more stable at higher pressures. Further investigating the amount of holes on the O-p orbitals, we find that with pressure the amount of charge on the oxygen ligand sites decreases monotonically. The charges were computed within the same radius, scaled to the reduction in volume, shown in Fig. SM-10. A decrease in the charges indicates an effective increase in the amount of O-p holes. The presence of such

holes can stabilize the ferromagnetic coupling between the Co sites, as shown in Fig. 3(b). Indeed, small local moments observed on the O-p sites ($0.17\,\mu_B$) had an opposite orientation to the ferromagnetically coupled moments on the Co site. This clearly suggests that the reduction in the band gap and its eventual closing under the application of pressure in the BM-SCO insulator is also driven by the same charge-transfer energy, with compressive (tensile) strain acting as a p (n)-doping of the system which thereby modifies the ligand holes, and that the AFM ordering in unstrained BM-SCO is a secondary effect that further assists in stabilizing the gap. Our findings also elucidate the physics underpinning recently observed machine-learning-based identification of the average deviation of covalent radii and the global instability index as features that predominantly correlate with the tendency of materials to undergo a thermally driven MIT [42].

III. CONCLUSIONS

In this work, we use density-functional-theory–based methods and the diffusion Monte Carlo (DMC) flavor of the many-body quantum Monte Carlo (QMC) approach that explicitly treats strong electron-electron correlations to understand what drives MIT in correlated perovskites. Where experimental data is available, comparisons of cohesive energies, local moments, and other quantities are made. We find the correlated metal such as PV-SCO and PV-LNO to be self-hole-doped as measured by significant Op contributions to conduction bands and decreased oxygen occupation relative to the studied insulators, with similar amounts of ligand hole. The electronic band gaps in insulating compounds that are related to these-self-hole doped metals via n doping, due to changes in oxygen stoichiometry such as $SrCoO_{2.5}$ or metal compositions such as $LaFeO_3$ and $LaCrO_3$, show filling of this ligand hole in some sites, with the gap nearly linearly changing with the degree of average (or majority) filling, suggesting that the band gap is opened by charge-transfer energies. Further, the insulating phases are shown to be *both* charge and bond disproportionated due to an underlying charge-lattice coupling, with more ligand holes on certain oxygen sites than others in the symmetry-lowered bond-disproportionated phase. The charge disproportionation drives bond disproportionation, as is seen from phonon instabilities that arise when n doping a pristine cubic perovskite phase. Together, this leads to the opening of a band gap that is more $p-d$-like beyond a critical amount of n doping, transitioning a self-hole-doped metal to a less self-hole-doped insulator. Similarly, we find that pressure leads to an increase in ligand holes in the oxygen sites, driving a transition to a ferromagnetic metallic ground state.

Our study thus suggests that self-hole-doped correlated metals can trigger a metal-to-insulator transition by n doping into a less self-hole-doped insulator, as doping makes the charge-transfer energy more positive, and that this can lead to symmetry-lowering transitions due to a strong charge-lattice (or electron-phonon) coupling. This n doping can be achieved by modulations in oxygen stoichiometry or metal composition or pressure. Moreover, this tendency to remain self-hole-doped in correlated metals determines a universal electronic response to modulations in oxygen stoichiometry/metal composition/pressure via the charge-lattice coupling. Hence, controlling the amount and anisotropy of the ligand hole is the key factor in controlling MIT even in correlated metals, and the band gap is fundamentally controlled by the strength of the charge-transfer energy close to the MIT and not by the Mott-Hubbard interactions, as originally thought for Mottronics applications [43]. While we do not present a rigorously predictive quantitative model that explains all of our observations, we have shown clearly that there exists a linear trend between the calculated band gaps and oxygen occupations across changes in composition, stoichiometry, or pressure. In addition, one could argue that the same trend would be seen for the hybridization between the transition metal and ligand site, which is related to the change in occupation; however, hybridization cannot be quantitatively measured in the solid state, so we use occupations as a proxy. This knowledge can be used to discover new materials where MIT can be controlled more reliably, enabling low-power and efficient neuromorphic devices [4].

ACKNOWLEDGMENTS

This work was supported by the U.S. Department of Energy, Office of Science, Basic Energy Sciences, Materials Sciences and Engineering Division, as part of the Computational Materials Sciences Program and Center for Predictive Simulation of Functional Materials. Part of this research (DFT calculations using VASP) was conducted at the Center for Nanophase Materials Sciences (CNMS), which is a DOE Office of Science User Facility. This research used resources of the Oak Ridge Leadership Computing Facility at the Oak Ridge National Laboratory, which is supported by the Office of Science of the U.S. Department of Energy under Contract No. DE-AC05-00OR22725. This research used resources of the National Energy Research Scientific Computing Center, a DOE Office of Science User Facility supported by the Office of Science of the U.S. Department of Energy under Contract No. DE-AC02-05CH11231. This manuscript has been authored by UT-Battelle, LLC under Contract No. DE-AC05-00OR22725 with the U.S. Department of Energy. The United States Government retains and the publisher, by accepting the article for publication, acknowledges that the United States Government retains a nonexclusive, paid-up, irrevocable, worldwide license to publish or reproduce the published form of this manuscript, or allow others to do so, for United States Government purposes. The Department of Energy will provide public access to these results of federally sponsored research in accordance with the DOE Public Access Plan.

M.C.B. and G.H. contributed equally to this work.

[1] Y. Zhou and S. Ramanathan, Mott memory and neuromorphic devices, Proc. IEEE **103**, 1289 (2015).

[2] J. L. Andrews, D. A. Santos, M. Meyyappan, R. S. Williams, and S. Banerjee, Building brain-inspired logic circuits from

dynamically switchable transition-metal oxides, Trends Chem. **1**, 711 (2019).

[3] S. Zhang and G. Galli, Understanding the metal-to-insulator transition in $La_{1-x}Sr_xCoO_{3-\delta}$ and its applications for neuromorphic computing, npj Comput. Mater. **6**, 170 (2020).

[4] K. Zhang, J. Wang, Y. Huang, L.-Q. Chen, P. Ganesh, and Y. Cao, High-throughput phase-field simulations and machine learning of resistive switching in resistive random-access memory, npj Comput. Mater. **6**, 198 (2020).

[5] M. Imada, A. Fujimori, and Y. Tokura, Metal-insulator transitions, Rev. Mod. Phys. **70**, 1039 (1998).

[6] G. Grüner, The dynamics of charge-density waves, Rev. Mod. Phys. **60**, 1129 (1988).

[7] U. Staub, G. I. Meijer, F. Fauth, R. Allenspach, J. G. Bednorz, J. Karpinski, S. M. Kazakov, L. Paolasini, and F. dAcapito, Direct Observation of Charge Order in an Epitaxial NdNiO 3 Film, Phys. Rev. Lett. **88**, 126402 (2002).

[8] M. Hepting, M. Minola, A. Frano, G. Cristiani, G. Logvenov, E. Schierle, M. Wu, M. Bluschke, E. Weschke, H. U. Habermeier, E. Benckiser, M. LeTacon, and B. Keimer, Tunable Charge and Spin Order in PrNiO 3 Thin Films and Superlattices, Phys. Rev. Lett. **113**, 227206 (2014).

[9] R. Scherwitzl, S. Gariglio, M. Gabay, P. Zubko, M. Gibert, and J.-M. Triscone, Metal-Insulator Transition in Ultrathin LaNiO 3 Films, Phys. Rev. Lett. **106**, 246403 (2011).

[10] Q. Lu and B. Yildiz, Voltage-controlled topotactic phase transition in thin-film SrCoO x monitored by in situ X-ray diffraction, Nano Lett. **16**, 1186 (2016).

[11] N. Lu, P. Zhang, Q. Zhang, R. Qiao, Q. He, H.-B. Li, Y. Wang, J. Guo, D. Zhang, Z. Duan *et al.*, Electric-field control of tri-state phase transformation with a selective dual-ion switch, Nature (London) **546**, 124 (2017).

[12] H. Jeen, W. S. Choi, M. D. Biegalski, C. M. Folkman *et al.*, Reversible redox reactions in an epitaxially stabilized SrCoO x oxygen sponge, Nat. Mater. **12**, 1057 (2013).

[13] W. S. Choi, H. Jeen, J. H. Lee, S. A. Ambrose Seo, V. R. Cooper, K. M. Rabe, and H. N. Lee, Reversal of the Lattice Structure in SrCoO x Epitaxial Thin Films Studied by Real-Time Optical Spectroscopy and First-Principles Calculations, Phys. Rev. Lett. **111**, 097401 (2013).

[14] F. Hong, B. Yue, Z. Liu, B. Chen, and H.-K. Mao, Pressure-driven semiconductor-semiconductor transition and its structural origin in oxygen vacancy ordered SrCo O 2.5, Phys. Rev. B **95**, 024115 (2017).

[15] S. Chowdhury, A. Jana, M. Kuila, V. R. Reddy, R. J. Choudhary, and D. M. Phase, Negative charge-transfer energy in $SrCoO_{2.5}$ thin films: An interplay between o-2p hole density, charge-transfer energy, charge disproportionation, and ferromagnetic ordering, ACS Appl. Electron. Mater. **2**, 3859 (2020).

[16] R. Jaramillo, S. D. Ha, D. Silevitch, and S. Ramanathan, Origins of bad-metal conductivity and the insulator–metal transition in the rare-earth nickelates, Nat. Phys. **10**, 304 (2014).

[17] V. Bisogni, S. Catalano, R. J. Green, M. Gibert, R. Scherwitzl, Y. Huang, V. N. Strocov, P. Zubko, S. Balandeh, J.-M. Triscone, G. Sawatzky, and T. Schmitt, Ground-state oxygen holes and the metal–insulator transition in the negative charge-transfer rare-earth nickelates, Nat. Commun. **7**, 13017 (2016).

[18] J. Shamblin, M. Heres, H. Zhou, J. Sangoro, M. Lang, J. Neuefeind, J. A. Alonso, and S. Johnston, Experimental evidence for bipolaron condensation as a mechanism for the metal-insulator transition in rare-earth nickelates, Nat. Commun. **9**, 86 (2018).

[19] J. B. Torrance, P. Lacorre, A. I. Nazzal, E. J. Ansaldo, and C. Niedermayer, Systematic study of insulator-metal transitions in perovskites R NiO 3 (R = Pr, Nd, Sm, Eu) due to closing of charge-transfer gap, Phys. Rev. B **45**, 8209 (1992).

[20] H. Guo, Z. W. Li, L. Zhao, Z. Hu, C. F. Chang, C.-Y. Kuo, W. Schmidt, A. Piovano, T. W. Pi, O. Sobolev, D. I. Khomskii, L. H. Tjeng, and A. C. Komarek, Antiferromagnetic correlations in the metallic strongly correlated transition metal oxide $LaNiO_3$, Nat. Commun. **9**, 43 (2018).

[21] J. Shi, Y. Zhou, and S. Ramanathan, Colossal resistance switching and band gap modulation in a perovskite nickelate by electron doping, Nat. Commun. **5**, 4860 (2014).

[22] H.-T. Zhang, F. Zuo, F. Li, H. Chan *et al.*, Perovskite nickelates as bio-electronic interfaces, Nat. Commun. **10**, 1651 (2019).

[23] J. Zaanen, G. A. Sawatzky, and J. W. Allen, Band Gaps and Electronic Structure of Transition-Metal Compounds, Phys. Rev. Lett. **55**, 418 (1985).

[24] I. Kylänpää, J. Balachandran, P. Ganesh, O. Heinonen, P. R. C. Kent, and J. T. Krogel, Accuracy of *ab initio* electron correlation and electron densities in vanadium dioxide, Phys. Rev. Materials **1**, 065408 (2017).

[25] I. Kylänpää, Y. Luo, O. Heinonen, P. R. C. Kent, and J. T. Krogel, Compton profile of VO_2 across the metal-insulator transition: Evidence of a non-Fermi liquid metal, Phys. Rev. B **99**, 075154 (2019).

[26] P. Ganesh, F. Lechermann, I. Kylänpää, J. T. Krogel, P. R. C. Kent, and O. Heinonen, Doping a bad metal: Origin of suppression of the metal-insulator transition in nonstoichiometric VO_2, Phys. Rev. B **101**, 155129 (2020).

[27] Q. Lu, C. Sohn, G. Hu, X. Gao *et al.*, Metal-insulator transition tuned by oxygen vacancy migration across TiO2/VO2 interface, Sci. Rep. **10**, 18554 (2020).

[28] H. Shin, Y. Luo, P. Ganesh, J. Balachandran, H. Shin, Y. Luo, P. Ganesh, J. Balachandran, J. T. Krogel, P. R. C. Kent, A. Benali, and O. Heinonen, Electronic properties of doped and defective NiO: A quantum Monte Carlo study, Phys. Rev. Materials **1**, 073603 (2017).

[29] F. Wrobel, H. Park, C. Sohn, H.-W. Hsiao, J. M. Zuo, H. Shin, H. N. Lee, P. Ganesh, A. Benali, P. R. C. Kent, O. Heinonen, and A. Bhattacharya, Doped NiO: The mottness of a charge transfer insulator, Phys. Rev. B **101**, 195128 (2020).

[30] P. C. Rogge, R. U. Chandrasena, A. Cammarata, R. J. Green, P. Shafer, B. M. Lefler, A. Huon, A. Arab, E. Arenholz, H. N. Lee, T. L. Lee, S. Nemsak, J. M. Rondinelli, A. X. Gray, and S. J. May, Electronic structure of negative charge transfer CaFeO 3 across the metal-insulator transition, Phys. Rev. Materials **2**, 015002 (2018).

[31] J. Kuneš, V. Křápek, N. Parragh, G. Sangiovanni, A. Toschi, and A. V. Kozhevnikov, Spin State of Negative Charge-Transfer Material SrCoO 3, Phys. Rev. Lett. **109**, 117206 (2012).

[32] R. Grimm and R. Storer, Monte-Carlo solution of Schrödinger's equation, J. Comput. Phys. **7**, 134 (1971).

[33] W. M. C. Foulkes, L. Mitas, R. J. Needs, and G. Rajagopal, Quantum Monte Carlo simulations of solids, Rev. Mod. Phys. **73**, 33 (2001).

[34] M. Cococcioni and S. de Gironcoli, Linear response approach to the calculation of the effective interaction parameters in the LDA+ U method, Phys. Rev. B **71**, 035105 (2005).

[35] See Supplemental Material at http://link.aps.org/supplemental/10.1103/PhysRevResearch.4.L022005 for the details of the DFT and QMC approaches that were used in this manuscript, figures show the nodal optimization result to obtain a QMC-benchmarked DFT-approach, QMC-derived cohesive energies for perovskite solids, phonon dispersions, as well as tables reporting material properties such as local magnetic moments, optical gaps and on-site charges, obtained from our QMC and/or QMC-benchmarked DFT-based calculations.

[36] A. Jain, G. Hautier, S. P. Ong, C. J. Moore, C. C. Fischer, K. A. Persson, and G. Ceder, Formation enthalpies by mixing GGA and GGA $+U$ calculations, Phys. Rev. B **84**, 045115 (2011).

[37] W. Koehler and E. Wollan, Neutron-diffraction study of the magnetic properties of perovskite-like compounds LaBO3, J. Phys. Chem. Solids **2**, 100 (1957).

[38] A. Muñoz, C. de la Calle, J. A. Alonso, P. M. Botta, V. Pardo, D. Baldomir, and J. Rivas, Crystallographic and magnetic structure of $SrCoO_{2.5}$ brownmillerite: Neutron study coupled with band-structure calculations, Phys. Rev. B **78**, 054404 (2008).

[39] M. D. Scafetta, Y. J. Xie, M. Torres, J. E. Spanier, and S. J. May, Optical absorption in epitaxial $La_{1-x}Sr_xFeO_3$ thin films, Appl. Phys. Lett. **102**, 081904 (2013).

[40] K. Maiti and D. D. Sarma, Electronic structure of $La_{1-x}Sr_xCrO_3$, Phys. Rev. B **54**, 7816 (1996).

[41] J. L. Cohn, Heat conduction and charge ordering in perovskite manganites, nickelates and cuprates, arXiv:cond-mat/0003047.

[42] A. B. Georgescu, P. Ren, A. R. Toland, S. Zhang, K. D. Miller, D. W. Apley, E. A. Olivetti, N. Wagner, and J. M. Rondinelli, Database, features, and machine learning model to identify thermally driven metal-insulator transition compounds, Chem. Mater. **33**, 5591 (2021).

[43] J. Chen, W. Mao, L. Gao, F. Yan *et al.*, Electron-doping mottronics in strongly correlated perovskite, Adv. Mater. **32**, 1905060 (2020).